JMEPEG (2005) 14:480-486
DOI: 10.1361/105994905X56160

1059-9495/$19.00

Using Differential Scanning Calorimetry to Characterize the Precipitation Hardening Phenomena in a Cu-9Ni-6Sn Alloy

N. Lourenço and H. Santos

(Submitted November 10, 2003; in revised form March 18, 2005)

An attempt has been made to characterize the transformations in a Cu-9Ni-6Sn alloy using heat flux differential scanning calorimetry (DSC) assisted by hardness measurements. Both solution heat treatment and precipitation transformations have been studied. Different starting conditions were imposed on the material to allow a clearer understanding of the transformations involved. The precipitation from the supersaturated solid solution happens in two temperature ranges, i.e., from 200 to 400 °C and from 440 to 600 °C. In the temperature range from 400 to 440 °C, the alloy does not usually transform. Thermal cycles leading to aging and overaging were determined. The precipitation hardening conditions at 350 °C or lower for less than 600 min, or 375 °C for up to 120 min, lead to metastable precipitation. Precipitation hardening for 120 min at 400 °C or 1200 min at 350 °C results in stable precipitation and is responsible for overaging the alloy.

Keywords: aging, Cu-9Ni-6Sn alloy, differential scanning calorimetry, precipitation hardening, solution treatment

1. Introduction

Copper alloys of the systems Cu-Ni-Sn, Cu-Be, and Cu-Ti have the potential to develop tensile strengths greater than 1000 MPa (Ref 1, 2). The Cu-Ti alloys are poorly documented, however. The Cu-Ni-Sn alloys may exhibit tensile strengths equal to those of high-strength precipitation hardened Cu-Be alloys but free from the health hazards and difficulties encountered in manufacturing Cu-Be alloys (Ref 3). The Cu-Ni-Sn alloys may be aggressive competitors to the Cu-Be alloys when high strength and high conductivity are required.

The Cu-Ni-Sn alloys achieve their maximum tensile strength through a processing sequence consisting of a solution heat treatment (to obtain a supersaturated state) followed by a precipitation hardening stage (to impose the required hardening by a controlled precipitation sequence).

In equilibrium conditions, the alloy becomes homogeneous at a temperature close to 750 °C, dependant on the solute content, and is composed of a disordered solid solution (α) of Ni and Sn in Cu with a face-centered cubic (fcc) crystal structure. Upon decreasing the temperature, the solubility of Ni and Sn in Cu decreases significantly, and a second phase is formed. This phase is the ordered γ phase with a $D0_3$ crystal structure. The solution heat treatment is followed by quenching, and this step is responsible for producing a supersaturated solid solution at room temperature, thus avoiding the formation of the γ phase. The controlled precipitation from the supersaturated solid solution during the precipitation hardening stage causes several transformations to occur. These transformations depend not only on the chemical composition of the alloy, but also on the thermo-mechanical processing of the alloy. The general sequence for these transformations proceeds as follows: (1) in a first stage, a spinodal decomposition occurs at temperatures lower than 500 °C; (2) later, a metastable precipitate is formed, that may crystallize as $D0_{22}$ (γ') and $L1_2$, both with a stoichiometry $(Cu_xNi_{1-x})_3Sn$; and (3) the equilibrium γ phase forms (Ref 1, 4-6).

Although Cu-9Ni-6Sn is referred in the literature as the one with the higher commercial potential, offering an excellent combination of electrical, thermal, chemical, and mechanical properties (Ref 1,7), its phase transformations are less well characterized than in other alloys like Cu-15Ni-8Sn and Cu-7.5Ni-5Sn. This was one reason this study was undertaken. In addition, the use of differential scanning calorimetry as a tool to characterize the phase transformations occurring during the thermal processing of the alloy was a second reason for this research because results obtained from this technique as applied to Cu-Ni-Sn alloys are unavailable in the literature.

2. Materials and Procedures

The material used in this study is a commercial Cu-9Ni-6Sn alloy, composition in weight percent, in the prehardened state (28-32 HRC or 328 $VHN_{2.94N}$).

2.1 Description and Procedures for Differential Scanning Calorimetry

Heat flux differential scanning calorimetry (DSC) was used in the study. All tests were run under a 1-3 bar Ar flux using cylindrical samples 3-3.5 mm in diameter and 1-2.5 mm in thickness. The samples had a mass from 50 to 200 mg. Alumina powder was used as the reference material.

N. Lourenço and **H. Santos,** Faculdade de Engenharia da Universidade do Porto (Engineering School of Porto University), DEMM/FEUP, R. Dr. Roberto Frias 4200-465 Porto, Portugal. Contact e-mail: nl@fe.up.pt and hsantos@fe.up.pt.

Table 1 Data relative to the determination of the calibration factor (K_T)

Standard material	Melting point(a), °C	Melting range, °C	Melting enthalpy(a), J/g	Sample mass, g	Area of the melting peak, μV s	Calibration factor, W/μV
In	157	155-164	28.4	60.6×10^{-3}	542.4	3.17×10^{-3}
Pb	327.5	325-335	24.7	49.1×10^{-3}	295.2	4.11×10^{-3}
Al	660	658-683	395.0	28.2×10^{-3}	2206.2	5.05×10^{-3}
Ag	962	958-970	104.5	50.1×10^{-3}	1281.3	4.09×10^{-3}

(a) Data collected from the Labsys Instruction Manual, SETARAM, 1999

DSC measures the temperature difference between the sample and the reference material, which is amplified and plotted (in μV). When the sample undergoes a transformation, it releases or absorbs heat. A calibration was run to convert this amplified voltage signal into power units, allowing the determination of the evolution of the specific heat capacity (C_p) of each sample during a test. Indium, lead, aluminum, and silver with purities greater than 99.99% were used as standards for the calibration (melting points of these metals are, respectively: 157, 327.5, 660 and 962 °C). The calibration factor (K_T) was calculated using the expression (Ref 8):

$$\Delta H = \frac{K_T \times S}{m} \quad \text{(Eq 1)}$$

where ΔH is the melting enthalpy of the standard metal (J/g), m is the mass of the sample (g), and S represents the area of the melting peak evaluated from the test. Because the melting of each standard metal occurs in a small temperature range, which may be converted into time view the constant heating rate imposed during the test, the units of the melting peak area become μV s. Three tests were run per standard metal with a 10 °C/min heating rate. The average results of the calibration tests are shown in Table 1, together with data necessary for the calibration factor determination (Ref 9). Using Eq 1 establishes the dependence of K_T (W/μV) with the temperature (°C):

$$K_T = 1.70 \times 10^{-3} + 1.03 \times 10^{-5} \times T - 8.15 \times 10^{-9} \times T^2 \quad \text{(Eq 2)}$$

which is valid in the temperature range 157–962 °C.

Knowing the calibration factor K_T, the value of the specific heat capacity, C_p, at a given temperature can be calculated from the signal obtained in the DSC curves using the equation:

$$C_p = \frac{q_s \times K_T}{dT/dt} \times (1/m) \quad \text{(Eq 3)}$$

where q_s is the y coordinate obtained from the test (μV), K_T is the calibration factor (W/μV), dT/dt is the heating rate during the test (°C/s), and m is the mass of the sample (g). C_p is expressed in J/°C g. The data presented in the next sections for the change of the specific heat capacity with temperature (C_p versus T) were determined in accordance with the previous procedure.

The DSC software calculates the energy associated with a peak directly from the test signal in μV s. This means that the aforementioned correction is not taken into account. To determine the peak energies in J/g wherever necessary in this work, the C_p versus T corrected curve integration was performed using the composed trapezoid rule.

Each DSC test was repeated at least once. This allowed determination of a range of values for any characteristic DSC trace resulting from the test.

2.2 Heat Treatment Procedures

To implement the solution heat treatment characterization, one group of samples was previously annealed (A) at 825 °C for 30 min, followed by slow cooling at 10 °C/h. The DSC tests consisted of heating these samples at several different rates to 875 °C. Heating should cause a progressive dissolution of the equilibrium phase until homogenization of the alloy occurs.

For the precipitation hardening studies, two groups of samples were prepared: (a) solution heat treated (SHT) at 825 °C for 30 min followed by fast cooling in water at 3 °C (selection of the SHT parameters will be explained later), and (b) precipitation hardened (PH) using different conditions, which will be described later. The DSC tests consisted of heating the samples to 875 °C; heating the *SHT* samples causes precipitation whereas heating the PH samples cause growth, or dissolution, of the precipitates, depending on their relative stability.

The dissolution start and finish temperatures for precipitates in the PH condition were generally identified with the onset and offset temperatures. In some cases, the onset temperature could not be used for this purpose because the procedure adopted in the thermal analysis study requires the intersection of two straight lines drawn in a temperature range lower and higher than the one corresponding to the maximum of the C_p versus T curve. This procedure causes strong variations in the onset temperature when the amplitude of the peak changes. In these cases, the first derivative of the C_p versus T curve was used to determine the dissolution start temperature of the precipitate.

To assess the degree of precipitation hardening in the alloy, hardness measurements were performed on samples, 10 mm on edge. These specimens were subjected to heat treatments in a muffle furnace using thermal parameters selected in accordance with the DSC results. Vickers hardness indents used a 2.94 N load applied during 15 s.

3. Results and Discussion

3.1 Annealed (A) and Solution-Treated (ST) Condition

The hardness values of the Cu-9Ni-6Sn alloy in the A and SHT conditions are presented in Table 2. Each hardness number is the mean of 50 indentations. The hardening effect from Ni and Sn in solid solution (i.e., SHT condition) is obvious relative to pure Cu. It is also clear that the equilibrium precipitation of γ during the slow cooling of the alloy (i.e., A condition) is responsible for considerable hardening of the material relative to the SHT state. The standard deviation of the hard-

Table 2 Hardness of samples in the A and SHT conditions (hardness of annealed Cu added for comparison)

Sample	Heat treatment	VHN/2.94N Mean	VHN/2.94N standard deviation
A	825 °C for 30 min and cooling at 10 °C/h	161	11
SHT	825 °C for 30 min and cooling in water at 3 °C	124	5
Cu	Annealed	60-82(a)	…

(a) Data obtained from http://properties.copper.org/ in the HRB scale and converted in accordance with George L. Kehl (Ref 10)

ness data of the samples in the A condition is about twice that of SHT condition. This aspect may be explained by the homogeneous state of the alloy in the SHT condition, where it is composed of supersaturated α. In the A condition, the alloy is composed of a mixture of quasi-equilibrium α and γ phases with different physical and mechanical characteristics. One may then conclude that the Ni and Sn solution hardening effect has been overcome by the moderate precipitation hardening of the equilibrium phase.

The DSC tests have been run on samples in the A condition to characterize the dissolution of the equilibrium phase at 25 and 35 °C/min heating rates. An example of these results is shown in Fig. 1. The γ phase dissolution is characterized by an endothermic peak.

The DSC tests on samples in the SHT condition have been run by continuously heating the test pieces to 875 °C at 25, 35, and 40 °C/min. Figure 2 shows the curve obtained for a 35 °C/min heating rate, where the exothermic peaks document the occurrence of precipitation in the two temperature regimes, i.e., from 200 to 400 °C and again from 440 to 600 °C.

Table 3 displays the results obtained from the DSC tests illustrated in Fig. 1. The dissolution of the equilibrium precipitate was assumed to start at the onset temperature and to be concluded at the offset temperature. This may be identified as the solvus point of the alloy for the heating rate imposed, above which the alloy becomes homogeneous. The γ precipitation is stable up to 620 °C for heating rates equal to, or greater than, 25 °C/min. The peak and offset temperatures increase with the heating rate, demonstrating the effect of thermal hysteresis. In pseudo binary equilibrium diagrams for the Cu-Ni-Sn alloys, Zhao and Notis (Ref 4, 5) determined a solvus point at 800 °C for Cu-15Ni-8Sn and 700 °C for Cu-7.5Ni-5Sn. The solvus equilibrium point of the Cu-9Ni-6Sn alloy should be intermediate between these two, but because results obtained in this study have used a nonequilibrium heating rate, it seems reasonable that the temperature at the conclusion of the equilibrium precipitate dissolution (i.e., the offset temperature in Table 3) should be higher than the solvus point determined by Zhao and Notis (Ref 4, 5). The soak for 30 min at 825 °C used to homogenize the samples in the A, SHT, and PH conditions was established in accordance with these results.

The results of DSC tests run on samples in the SHT condition, illustrated in Fig. 2, are summarized in Table 4. Results indicate that precipitation has occurred in two different temperature ranges, each one associated with an exothermic peak. It is proposed that the lower temperature range (i.e., from 200 to 400 °C) corresponds to the formation of the metastable

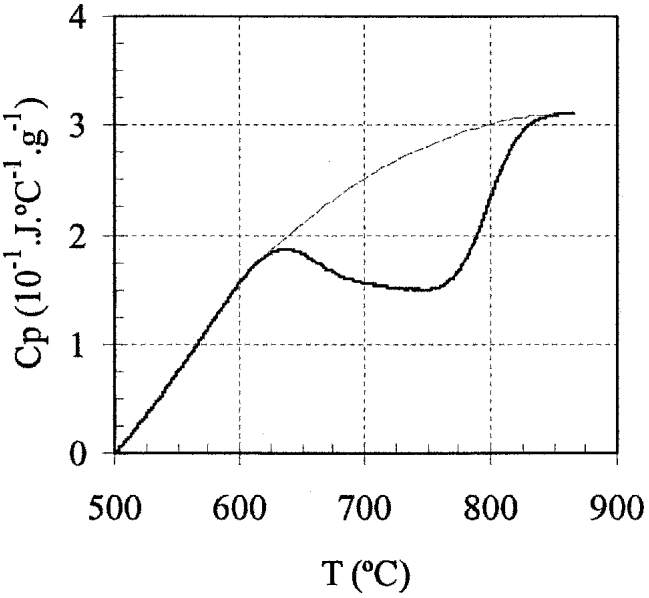

Fig. 1 Data obtained from a DSC test run at a 35 °C/min heating rate on a previously annealed sample; the baseline is represented by the lighter curve; the endothermic peak corresponds to the dissolution of the equilibrium phase. Curves have been set to zero at 500 °C.

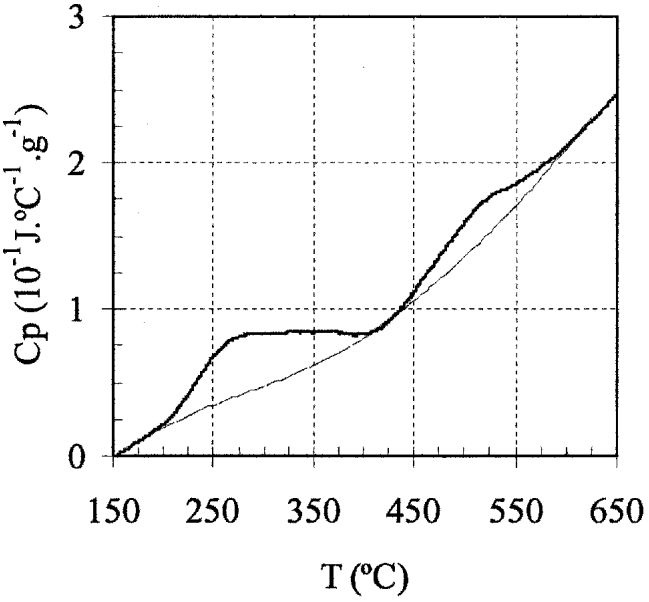

Fig. 2 Data obtained from a DSC test run at a 35 °C/min heating rate on a previously solution treated sample; the baseline is represented by the lighter curve; the exothermic peaks denounce precipitation phenomena in two ranges of temperatures. Curves have been set to zero at 150 °C.

precipitates whereas the higher temperature range (i.e., from 440 to 600 °C) is associated with the development of the equilibrium precipitate. These results are in good agreement with Zhao and Notis observations (Ref 5) because these authors present a TTT diagram for a Cu-7.5Ni-5Sn with a nonprecipitation domain around 450 °C. This behavior was observed in the current study for the Cu-9Ni-6Sn alloy, a finding that may be useful if a continuous heating procedure is adopted to harden the alloy. Because a broad process window occurs for

Table 3 Results from DSC solution treatment tests (illustrated in Fig. 1) of samples in the A condition

Heating rate, °C/min	Onset temperature, °C	Peak temperature, °C	Offset temperature, °C
25	620-634	743-749	813-820
35	624-629	759-763	825-830

Table 4 Characteristics of exothermic peaks (illustrated in Fig. 2) obtained from DSC tests in the SHT condition

Exothermic peak	Heating rate, °C/min	Onset temperature, °C	Peak temperature, °C	Offset temperature, °C
1st	35	198-211	267-268	391-399
	40	215-219	267-275	400-402
2nd	35	439-447	508-516	551-559
	40	486-492	516-532	584-598

the metastable precipitation, which is responsible for the maximum hardening effect, and because no precipitation occurs from 400 to 440 °C, temperature control for precipitation hardening of the alloy is not critical.

The temperature range for the equilibrium precipitate formation, i.e., lower than 600 °C, is also in good agreement with data obtained from the SHT study, given that the dissolution start temperature of the equilibrium precipitate is 620 °C.

3.2 PH Condition

Previous heat treatment of the samples consisted of the following: one group was subjected to SHT at 825 °C for 30 min followed by fast cooling in water at 3 °C, followed by isothermal aging at 300, 350, 360, 375, 400, and 450 °C for 120 min; and a second group was subjected to the same SHT, followed by isothermal aging at 350 °C for 15, 120, 600, and 1200 min. Figures 3 and 4 show examples of the DSC results obtained from these samples. The results show in all cases but one (i.e., case f in Fig. 3) that the isothermal transformation caused precipitation because dissolution of this previous precipitate is characterized by endothermic peaks.

The PH effect caused by the aging treatments was measured on samples subjected to the same thermal cycles described above. Results from these measurements are shown in Fig. 5 and 6, and in both cases overaging is demonstrated by a peak hardness followed by a hardness decrease.

Figures 3 and 4 show the DSC results obtained from the tests run on samples in the PH condition. The characteristics resulting from these tests are summarized in Tables 5 and 6.

With the exception of case (f) in Fig. 3, all curves have a similar shape and confirm dissolution of the precipitate previously formed. The curve for case (f) in Fig. 3, corresponding to a test run on a sample previously aged at 450 °C for 120 min, agrees with data presented in Fig. 2. No relevant dissolution phenomenon was detected, confirming the nonoccurrence of precipitation during previous aging. A verification of the nonoccurrence of precipitation in case (f) may be found in the hardness of the sample subjected to the same thermal cycle. If precipitation at 450 °C does not occur, the sample hardness should be identical to the one in the SHT condition. The average hardness of the sample aged at 450 °C for 120 min is 115 $VHN_{2.94N}$, which is quite close to the 124 $VHN_{2.94N}$ for the sample in the SHT condition.

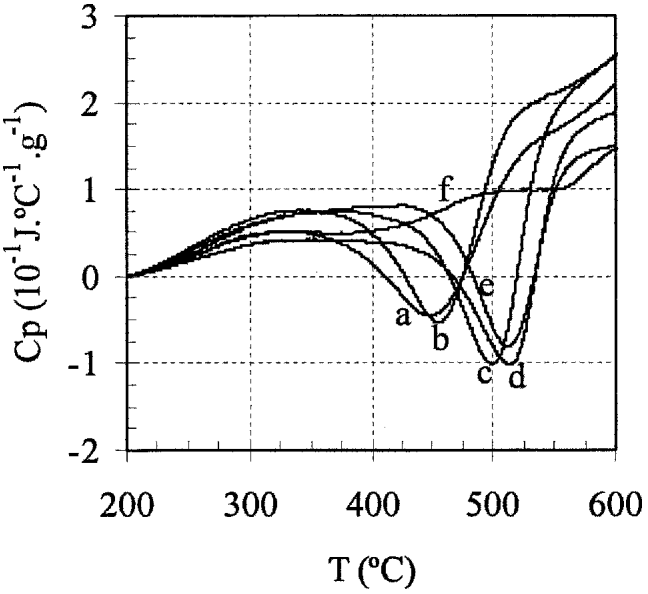

Fig. 3 Corrected DSC signal from tests run at a 35 °C/min heating rate on previously solution treated and aged samples during 120 min at (a) 300, (b) 350, (c) 360, (d) 375, (e) 400, and (f) 450 °C; in all cases but (f) endothermic peaks denounce the dissolution of the precipitates formed during previous aging. Curves have been set to zero at 200 °C.

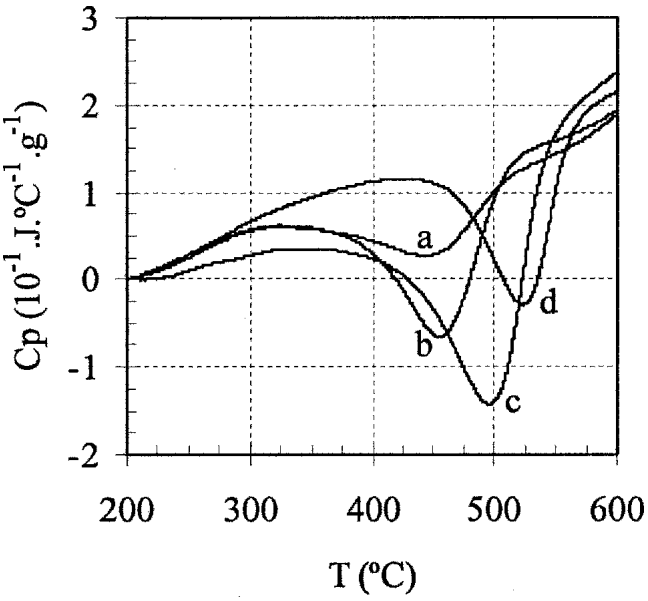

Fig. 4 Corrected DSC signal from tests run at a 35 °C/min heating rate on previously solution treated and aged samples at 350 °C for (a) 15, (b) 120, (c) 600, and (d) 1200 min; the endothermic peaks denounce the dissolution of the precipitates formed during previous aging. Curves have been set to zero at 200 °C.

For all other tests whose results are presented in Fig. 3 and 4, verification that the dissolution start temperature is lower than 620 °C was obtained. This is summarized in Tables 5 and 6. It was enhanced above that equilibrium precipitation is stable up

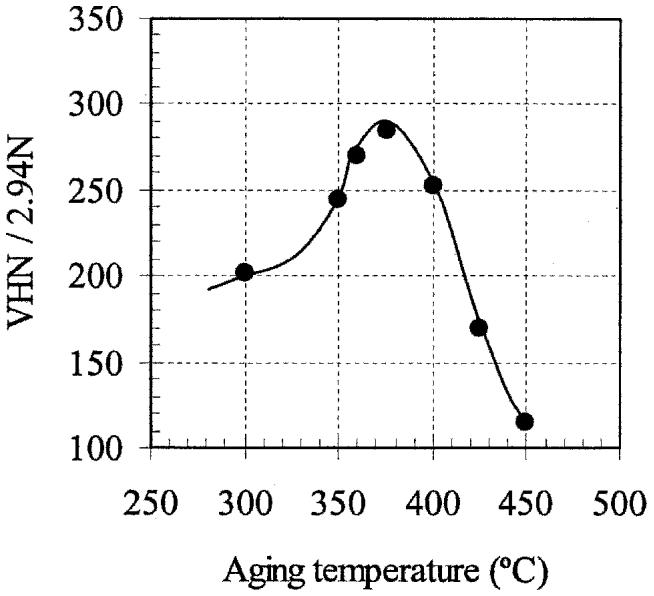

Fig. 5 Hardness of the precipitation hardened samples versus aging temperature at constant time (120 min)

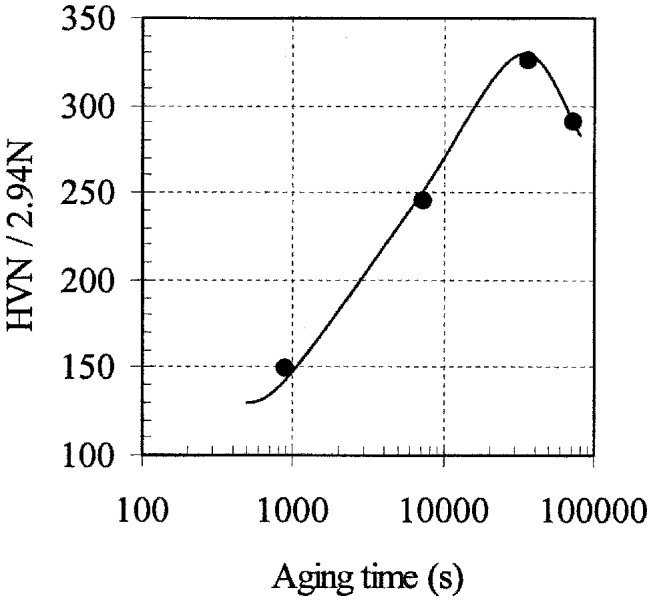

Fig. 6 Hardness of the precipitation hardened samples versus aging time at constant temperature (350 °C)

to 620 °C. One may then establish that when dissolution of precipitation is evident at temperatures lower than 620 °C in DSC tests, a metastable precipitation is detected.

This helps clarify the results from the DSC tests on the PH samples. When the aging conditions promote the formation of an increased fraction of metastable precipitates, the start, peak, and finish dissolution temperatures should tend to increase, and the dissolution energy associated with a DSC peak should also increase. When the aging conditions promote the formation of stable precipitates, the metastable precipitation fraction decreases because some of them transform into equilibrium precipitates. Thus, the start, peak, and finish dissolution temperatures tend to increase but the dissolution energy associated to a DSC peak should decrease. Tables 5 and 6 show that the dissolution energy increases for samples heat treated at 375 °C for an aging duration of 120 min and 600 min for an aging temperature of 350 °C. Precipitation hardening conditions exceeding the parameters defined above should promote overaging. This interpretation is partially confirmed by the hardness results presented in Fig. 5 and 6. As a result of these measurements, a correlation between hardness and the energy associated with a dissolution peak in the PH samples was evident. Indeed, a higher fraction of metastable precipitation should be responsible for the higher hardness. As such, the hardness of the PH samples is plotted in Fig. 7 against the average energy associated with the dissolution peak. An extra point was added to the data presented above, the result of a DSC test on the alloy in the commercial condition. Similarity was found between the DSC outputs from these tests and the ones resulting from the PH sample at 350 °C for 600 min. Figure 7 illustrates that a second order polynomial correlates well with the parameters (i.e., 0.92).

Table 5 Characteristics of endothermic peaks (illustrated in Fig. 3) obtained from DSC tests in the PH condition (SHT and aged for 120 min at indicated temperature) at a 35 °C/min

Aging temperature, °C	Dissolution start, °C	Maximum dissolution, °C	Dissolution finish, °C	Energy of dissolution peak, J/g
300	329-333	456-457	516-518	12.5-13.8
350	341-345	459-467	510-516	12.0-15.2
360	373-393	502-504	540-547	15.2-19.8
375	322-354	517-518	556-556	16.8-17.9
400	422-426	516-519	560-563	13.7-13.9

Table 6 Characteristics of endothermic peaks (illustrated in Fig. 4) obtained from DSC tests in the PH condition (SHT and aged for indicated time at 350 °C) at a 35 °C/min

Aging time, min	Dissolution start, °C	Maximum dissolution, °C	Dissolution finish, °C	Energy of dissolution peak, J/g
15	307-334	453-455	508-511	7.8-10.3
120	341-345	459-467	510-516	12.0-15.2
600	337-345	502-505	543-546	19.5-26.9
1200	409-419	526-526	565-565	13.3-14.8

Aging for 120 min at 375 °C, or lower (i.e., cases a-d in Fig. 3), and no more than 600 min at 350 °C (cases a-c in Fig. 4) are then responsible for producing mainly metastable precipitates. Aging for 120 min at 400 °C (case e in Fig. 3) and 1200 min at 350 °C (case d in Fig. 4) are responsible for coarsening the precipitates and transforming them into equilibrium precipitates. This is why the dissolution peak temperature increased and the peak energy decreased (i.e., a smaller fraction of coarser metastable precipitates dissolved).

According to the data presented above, continuous heating of the PH samples to 600 °C should promote the dissolution of the metastable precipitates. The stable precipitates should be relatively unaffected at these conditions. The hardness of the samples subjected to these conditions should be close to that in the SHT condition if mainly metastable precipitates are present. If a considerable fraction of stable precipitates are present

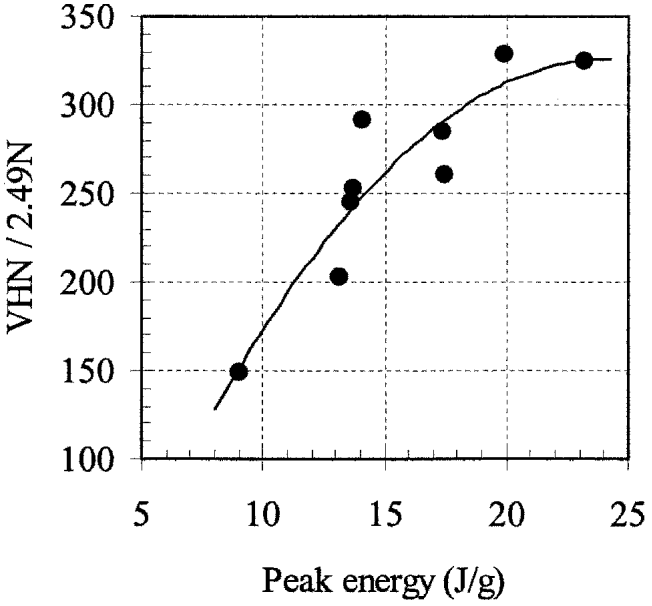

Fig. 7 Hardness versus energy of the dissolution peak calculated from the DSC tests of the precipitation hardened samples

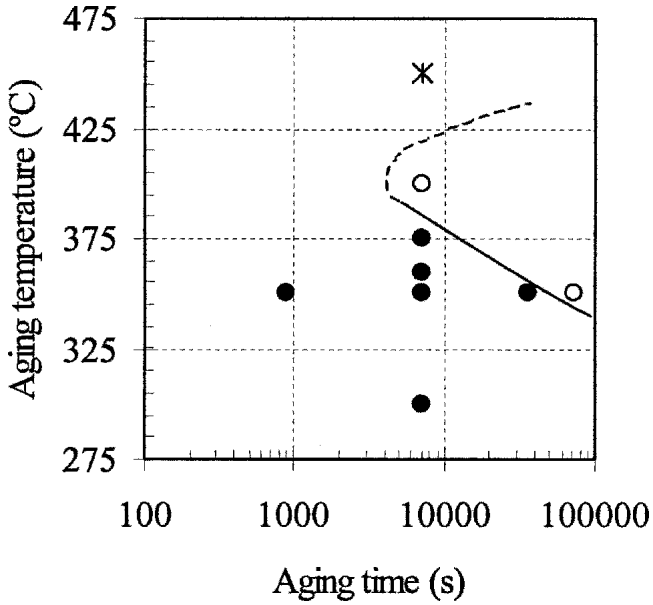

Fig. 8 Section of a TTT diagram obtained from the results of DSC and hardness tests for the decomposition of the supersaturated solid solution of the Cu-9Ni-6Sn alloy. Black circles represent the metastable precipitation, white circles represent the stable precipitation, and the cross represents the non-occurrence of precipitation. The solid line delineates the conditions responsible for the transition from metastable to stable precipitation.

(i.e., overaged state), dissolution will be incomplete, and the final hardness will be higher than the one observed in the SHT sample. Some samples were heat treated in a furnace in conditions similar to PH but with the addition of continuous heating to 600 °C at 20 °C/min. This is followed by cooling in water at 3 °C. The hardness of these samples is shown in Tables 7 and 8. It is clear that the precipitation hardening conditions of 400 °C for 120 min and 350 °C for 1200 min do not match the hardness of the sample in the SHT condition. However, all other aging conditions do, so it may be argued that a substantial fraction of stable precipitates arises from those conditions whose dissolution requires a temperature higher than 620 °C. The hardness of the samples aged for 120 min at 400 °C or for 1200 min at 350 °C, and reheated to 600 °C yield hardness values of 178 and 162 $VHN_{2.94N}$, respectively. These hardness values are close to the hardness of the A condition sample (i.e., 161 $VHN_{2.49N}$), indicating a considerable fraction of the equilibrium precipitates remain in all of them.

Summarizing the results from this work leads to the following observations:

- An isothermal heating stage of the supersaturated solid solution for no more than 120 min at 375 °C, or 600 min at 350 °C, leads to metastable precipitation;
- An isothermal heating stage of the supersaturated solid solution at 400 °C for 120 min, or 350 °C for 1200 min, leads to overaging, with stable precipitation; and,
- An isothermal heating stage of the supersaturated solid solution at 450 °C for 120 min does not promote any transformation.

Subsequently, a branch of the transformation-temperature-time (TTT) diagram for the Cu-9Ni-6Ni alloy can be plotted, showing the conditions leading to the transition from the metastable to the stable precipitation. This TTT diagram section is presented in Fig. 8. The results are consistent with the ones presented by Zhao and Notis (Ref 4, 5) in the studies on Cu-15Ni-8Sn and Cu-7.5Ni-5Sn. It was expected that the decomposition

Table 7 Hardness of the samples in the PH condition (SHT and aged for 120 min at indicated temperature) and reheated to 600 °C

Aging temperature, °C	$VHN_{2.94N}$
300	123
350	116
400	178
450	128

Table 8 Hardness of the samples in the PH condition (SHT and aged for indicated time at 350 °C) and reheated to 600 °C

Aging time, min	$VHN_{2.94N}$
15	118
120	116
600	129
1200	162

kinetics of the Cu-9Ni-6Sn alloy should be intermediate between those alloys because the solute content is also intermediate. Zhao and Notis showed (Ref 5) that the equilibrium precipitation from a Cu-7.5Ni-5Sn alloy occurs only at temperatures higher than the one that defines the stability bay of the supersaturated solid solution (i.e., 450 °C). However, this work was limited to isothermal heat treatments of 10^4 s in the temperature range from 300 to 450 °C. In the present work, isothermal heat treatments for up to 7.2×10^4 s (1200 min) have been run, and indeed, for heat treatment times up to 10^4 s, no equilibrium precipitation was detected. It is only for those times greater than 3.6×10^4 s and shorter than $7.2 \times$

10^4 s that the transition from metastable to stable precipitation has been identified. In their study of a Cu-15Ni-8Sn alloy, Zhao and Notis (Ref 4) suggested that equilibrium precipitation may occur at temperatures lower than the one defined by the stability bay of the supersaturated solid solution (i.e., around 500 °C in this case), if the isothermal heat treatment stage reaches 10^6 s in duration. This is in full agreement with the present results.

Finally, the DSC tests showed the capability of analyzing the precipitation response of the Cu-9Ni-6Sn alloy for different heat treatment conditions.

4. Conclusions

- The SHT ($\alpha + \gamma \rightarrow \alpha$) of Cu-9Ni-6Sn requires a minimum temperature of 820 °C if a 25 °C/min heating rate is not exceeded. Homogenizing at 830 °C is advised if the heating rate is increased to 35 °C/min.
- During continuous heating of A condition material, the equilibrium γ phase goes into solution at approximately 620 °C.
- The precipitation phenomenon during continuous heating of the supersaturated solid solution of Cu-9Ni-6Sn occurs in two temperature ranges: 200-400 °C and 440-600 °C. The lower range is responsible for a metastable precipitation, and the higher range promotes equilibrium precipitation.
- Cu-9Ni-6Sn is not prone to transformation at temperatures in the range from 400 to 440 °C, ensuring a process window that may be useful in industrial practice if continuous heating controlled precipitation is adopted as the processing sequence.
- Precipitation hardening at 350 °C for times up to 600 min, or 375 °C for times up to 120 min, leads to metastable precipitation, resulting in peak hardness. Precipitation hardening at 350 °C for 1200 min, or 400 °C for 120 min, results in an alloy that is "overaged."

Acknowledgment

The authors thank Dr. José Catita from PARALAB for the kind help with heat flux DSC operation.

References

1. J. Plebes, High Strength Cu-Ni-Sn Alloys by Thermomechanical Processing, *Metall. Trans.,* Vol 6A, 1975, p 537-544
2. S. Nagarjuna, K. Balasubramanian, and D.S. Darma, Effects of Cold Work on Precipitation Hardening of Cu-4.5 Mass % Ti Alloy, *Mater. Trans. JIM,* Vol 36 (No. 8), 1995, p 1058-1066
3. J. Rhu, S. Kim, Y. Yung, S. Han, and C. Kim, Tensile Strength of Thermomechanically Processed Cu-9Ni-6Sn Alloys, *Metall. Mater. Trans.,* Vol 30A, 1999, p 2649-2657
4. J. Zhao and M. Notis, Spinodal Decomposition, Ordering Transformation and Discontinuous Precipitation in a Cu-15Ni-8Sn Alloy, *Acta Mater.,* Vol 46 (No. 12), 1998, p 4203-4218
5. J. Zhao and M. Notis, Microstructure and Precipitation Kinetics in a Cu-7.5Ni-5Sn Alloy, *Scr. Mater.,* Vol 39 (No. 11), 1998, p 1509-1516
6. B. Ditchek and L. Schwartz, Diffraction Study of Spinodal decomposition in Cu-10 w/o Ni-6 w/o Sn, *Acta Metall.,* Vol 28, 1980, p 807-822
7. S. Kim, J. Rhu, Y. Yung, S. Han, and C. Kim, Aging Characteristics of Thermomechanically Processed Cu-9Ni-6Sn Alloy, *Scr. Mater.,* Vol 40 (No. 1), 1999, p 1-6
8. M.E. Brown, *Introduction to Thermal Analysis, Techniques and Applications,* 1st ed., Chapman and Hall, 1988, p 33
9. Labsys Instruction Manual, SETARAM, 1999
10. G.L. Kehl, *Principles of Metallographic Laboratory Practice,* 3rd ed., McGraw Hill Book Company, 1949, p 471